The hitting time density for a reflected Brownian motion

Qin Hu[†], Yongjin Wang[‡] and Xuewei Yang[†,1]
[†]School of Mathematical Sciences and TEDA Institute of Computational Finance, Nankai University, Tianjin 300071, P.R. China
[‡]School of Business, Nankai University, Tianjin 300071, P.R. China

Accepted for publication by ***Computational Economics*** on March 10, 2011

Abstract

Reflected Brownian motion has been played an important role in economics, finance, queueing and many other fields. In this paper, we present the explicit spectral representation for the hitting time density of the reflected Brownian motion with two-sided barriers, and give some detailed analysis on the computational issues. Numerical analysis reveals that the spectral representation is more appealing than the method of numerical Laplace inversion. Two applications are included at the end of the paper.

Key words: Reflected Brownian motion; hitting time; distribution function; density function; spectral representation; bankrupt probability; defaultable bond.

1. Introduction

Reflected Brownian motion (RBM) was first proposed as approximations of the queueing systems (see, e.g., Harrison (1978) and Harrison (1985)). It has been played an important role in economics, finance, queueing theory, and many other fields. For a comprehensive review of the vast literature on the theory and the applications of the RBM, please refer to Veestraeten (2004) and Linetsky (2005).

The study of the first hitting time of RBM is important both in itself and its applications in queueing, finance, insurance and many other fields (see, e.g., Kent (1980), Williams (1992), Werner (1995), Gerber and Shiu (2004), Bo, Zhang and Wang (2006), Veestraeten (2008), Bo et al. (2010), Bo, Wang and Yang (2011) and Bo et al. (2011)). Specifically, the Laplace transform of the first hitting time for a RBM has been documented by many authors (see, e.g.,

[1]Corresponding author at: School of Mathematical Sciences, Nankai University, Tianjin 300071, PR China. e-mail:xwyangnk@yahoo.com.cn

Williams (1992), Gerber and Shiu (2004) and Bo, Wang and Yang (2010, 2011)). However, to the best of our knowledge, the explicit representation for the hitting time density of RBM is still unavailable.

In this paper, we are concerned with the spectral expansion of the distribution function and the density function for the hitting time of the RBM. The general theory for spectral expansions of the diffusion hitting times was studied by Kent (1980, 1982). Recently, Linetsky (2004*b*) obtained the spectral decomposition for the hitting time of the CEV diffusion, which in turn resulted in the analytical representations for the lookback options. The same approach was applied to get the spectral decomposition of the hitting time densities for the CIR and OU diffusions in Linetsky (2004*a*). Essentially, all of these papers adopted the Sturm-Liouville spectral expansion technique discussed in McKean (1956).

We will present the detailed analysis on the computational issues for the spectral expansion of the hitting time density for the RBM. An advantage of the spectral expansion is that it is a global method (compared to the numerical Laplace inversion approach, which can only calculate the density function at some discrete points). The numerical analysis in this paper reveals that, specialized on the RBM case, the spectral representation is more appealing than the method of numerical Laplace inversion.

The last part of the paper concentrates on the applications of the theoretical results. Two applications are considered. The first follows the settings in Gerber and Shiu (2004), i.e., we model the (post-dividend) surplus process of an insurance company by the drifted Brownian motion with reflection. Then we present the distribution of the bankrupt time. The second partially follows the settings in Black and Cox (1976) and Veestraeten (2008): we model the market value of a firm by the geometric reflected Brownian motion. We then consider the pricing of a zero-recovery corporate (defaultable) bond, which is closely related to the distribution of the hitting time.

The paper is organized as follows: In the coming section, some preliminaries are given. In Section 3, we achieve the spectral expansion for the hitting time density. Both of the down hitting and the up hitting cases are studied. Section 4 concentrates on the numerical results for the convergence issues, where we also compare the spectral expansion approach with numerical Laplace inversion. Tow applications of our results are presented in Section 5: the first is to compute the distribution of the bankrupt time for an insurance company; the second is pricing a zero-recovery defaultable bond. Section 6 concludes the paper.

2. Preliminaries

In this paper, we consider the following RBM with two-sided reflecting barriers:[2]

$$\begin{cases} dX_t = \mu dt + \sigma dW_t + dL_t - dU_t, \\ X_0 = v \in [0,r], \end{cases} \tag{2.1}$$

where $W = (W_t)_{t\geq 0}$ is a standard Brownian motion, $\mu \in R$, and $\sigma > 0$. L and U are two regulators having the following properties (see, e.g., Harrison (1985)) :

(1) L and U are increasing and continuous with $L_0 = U_0 = 0$,

(2) $X_t \in [0,r]$ for all $t \geq 0$,

(3) L and U increase only when $X = 0$ and $X = r$, respectively.

The infinitesimal generator of the RBM is

$$(\mathcal{G}u)(x) := \frac{1}{2}\sigma^2 u''(x) + \mu u'(x), \quad x \in [0,r], \tag{2.2}$$

with the domain of definition given by

$$\mathcal{D}(\mathcal{G}) := \left\{ u \in C_b^2([0,r]); u'(0) = u'(r) = 0 \right\}. \tag{2.3}$$

The infinitesimal generator can be rewritten in the following symmetric form

$$(\mathcal{G}u)(x) = \frac{1}{m(x)} \left(\frac{u'(x)}{s(x)} \right)', \quad x \in [0,r], \tag{2.4}$$

where $s(x)$ and $m(x)$ are the diffusion scale and speed densities:

$$s(x) := \exp\left(-\frac{2\mu x}{\sigma^2} \right), \quad m(x) := \frac{2}{\sigma^2} \exp\left(\frac{2\mu x}{\sigma^2} \right). \tag{2.5}$$

It is not hard to verify that both of the boundaries 0 and r are regular instantaneously reflecting boundaries (see, e.g., Section 15.6 in Karlin and Taylor (1981)), which yield the boundary conditions in (2.3).

3. The distribution of the hitting time

In this section, we are mainly concerned with the distribution of the hitting time defined by

$$\tau := \inf\{t > 0;\ X_t = d\}, \tag{3.1}$$

[2]Here we only consider the case with lower boundary 0. The results for general cases can be obtained by a simple shift transform.

where $d\in[0,r]$ is the hitting level. In the following, we will deal with the cases $d\in[0,v)$ and $d\in(v,r]$ respectively. Note that the case $d=v$ is trivial.

3.1. Hitting down

In this subsection, we presume $d\in[0,v)$. To derive the spectral expansion of the density function of τ, we need to study the following Sturm-Liouville (SL) equation (see, e.g., Linetsky (2004*a*)):

$$\begin{cases} -\mathcal{G}u=\lambda u, \\ u'(r)=0. \end{cases} \tag{3.2}$$

The unique (up to a multiple independent of x) non-trivial solution of the above SL equation is:

$$\phi(x,\lambda)=\mu^{+}(\lambda)e^{\frac{\mu^{-}(\lambda)(r-x)}{\sigma^2}}-\mu^{-}(\lambda)e^{\frac{\mu^{+}(\lambda)(r-x)}{\sigma^2}}, \tag{3.3}$$

with $\mu^{\pm}(\lambda):=\mu\pm\sqrt{\mu^2-2\lambda\sigma^2}$. Moreover, if $\mu=0$, the above solution reduces to

$$\phi(x,\lambda)=\cos\left(\sqrt{\frac{2\lambda}{\sigma^2}}(r-x)\right). \tag{3.4}$$

Now we have the following

Proposition 3.1. *The distribution of the hitting time is given by*

$$\mathbb{P}_v(\tau\le t)=1-\sum_{n=1}^{\infty}c_n e^{-\lambda_n t},\quad t>0, \tag{3.5}$$

where $0<\lambda_1<\lambda_2<\cdots,\lambda_n\to\infty$ can be found as simple positive zeros of the function $\phi(d,\lambda)$, and c_n-s are explicitly given below:

$$c_n=\frac{-\phi(v,\lambda_n)}{\lambda_n\phi_\lambda(d,\lambda_n)},\quad n=1,2,\ldots. \tag{3.6}$$

Moreover, it must be hold that (see Tables 1-4 below)

$$\sum_{n=1}^{\infty}c_n=1. \tag{3.7}$$

Remark 3.2. *If $\mu=0$, the λ_n-s (the positive solutions to $\phi(d,\lambda)=0$) are given by*

$$\lambda_n=\frac{(2n-1)^2\sigma^2\pi^2}{8(r-d)^2}, \tag{3.8}$$

and the c_n-s are given by

$$c_n=\frac{(-1)^{n+1}4}{(2n-1)\pi}\cos\left(\frac{(2n-1)\pi}{2}\times\frac{r-v}{r-d}\right). \tag{3.9}$$

Due to the above results, when $\mu=0$, we can differentiate (3.5) to obtain the density function of the hitting time. In the following, we will concentrate on the general cases, i.e., $\mu\neq 0$.

In order to obtain the density function for the cases $\mu\neq 0$, we need some estimates on the λ_n-s and c_n-s. To this end, we will deal with the following equation in three different cases

$$\phi(d,\lambda)=0, \quad \lambda>0. \tag{3.10}$$

In the following, we only consider the case $\mu>0$. The result for the case $\mu<0$ can be obtained by a simple transform (see Remark 3.6 at the end of this section).

Case (I): $\lambda=\frac{\mu^2}{2\sigma^2}$.

It is easy to see that $\lambda_0:=\frac{\mu^2}{2\sigma^2}$ is a positive root to the equation (3.10) and $\phi(x,\lambda_0)\equiv 0$ for $x\in[0,r]$. Moreover, it is not hard to verify that (see also Figure 1)

$$\lim_{\lambda\to\lambda_0}|\phi_\lambda(d,\lambda)|=\begin{cases}+\infty, & \frac{\sigma^2}{\mu(r-d)}\neq 1,\\ 0, & \frac{\sigma^2}{\mu(r-d)}=1.\end{cases} \tag{3.11}$$

We thus have

$$c_0=\frac{-\phi(v,\lambda_0)}{\lambda_0\phi_\lambda(d,\lambda_0)}=0, \quad \text{for} \quad \frac{\sigma^2}{\mu(r-d)}\neq 1, \tag{3.12}$$

which means that the positive root $\lambda_0=\frac{\mu^2}{2\sigma^2}$ contributes nothing to the distribution function of the hitting time when $\frac{\sigma^2}{\mu(r-d)}\neq 1$. For the case $\frac{\sigma^2}{\mu(r-d)}=1$, c_0 (should be found by L'Hôpital's rule) may not be zero (see also Table 3).

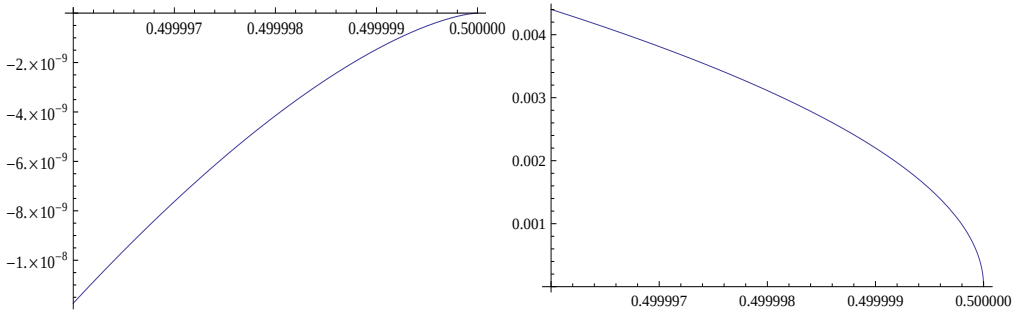

Figure 1: LEFT: $\phi(d,\lambda)$ with $d=1/4$, $\mu=1/4$, $\sigma=\sqrt{3}/4$, $r=1$, and $\frac{\sigma^2}{\mu(r-d)}=1$. RIGHT: $\phi_\lambda(d,\lambda)$ with the same parameters in the left panel.

Case (II): $\lambda\in(0,\frac{\mu^2}{2\sigma^2})$.

In this case, we have $\mu^2-2\lambda\sigma^2>0$. Define $x:=\sqrt{\mu^2-2\lambda\sigma^2}\in(0,\mu)$. Then the equation (3.10) can be rewritten as

$$f(x):=\frac{\sigma^2}{2(r-d)}\ln\left(\frac{\mu+x}{\mu-x}\right)=x. \tag{3.13}$$

Since $f(0)=0$, $f'(x)=\frac{\mu\sigma^2}{(r-d)}\frac{1}{\mu^2-x^2}$, $x\in(0,\mu)$ is a strictly increasing function, $f'(0+)=\frac{\sigma^2}{\mu(r-d)}$ and $f'(\mu-)=+\infty$, it follows that the equation (3.13) has a unique solution on $(0,\mu)$ if and only if $\frac{\sigma^2}{\mu(r-d)}<1$. If the unique solution exists, we denote it by x_0. Then the corresponding eigenvalue is given by $\lambda_{10}:=\frac{\mu^2-x_0^2}{2\sigma^2}$.

Case (III): $\lambda\in(\frac{\mu^2}{2\sigma^2},+\infty)$.

In this case, we have $\mu^2-2\lambda\sigma^2<0$. Define $\alpha:=\frac{r-d}{\sigma^2}\sqrt{2\lambda\sigma^2-\mu^2}\in(0,+\infty)$. By some standard calculus, the equation (3.10) can be rewritten as

$$\tan\alpha=\frac{\sigma^2}{\mu(r-d)}\alpha. \tag{3.14}$$

Denote the unique solution to the above equation in the interval $((n-1)\pi,(n-1)\pi+\pi/2)$ by α_n, for $n\geq 2$. Then $\lambda_n=\frac{\alpha_n^2\sigma^2}{2(r-d)^2}+\frac{\mu^2}{2\sigma^2}$, for $n\geq 2$. Moreover, it is easy to see that there is a unique solution to the above equation (3.14) in the interval $(0,\pi/2)$ if and only if $\frac{\sigma^2}{\mu(r-d)}>1$. If the unique solution in the interval $(0,\pi/2)$ exists, we denote it by α_1. Then the corresponding eigenvalue is given by $\lambda_{11}:=\frac{\alpha_1^2\sigma^2}{2(r-d)^2}+\frac{\mu^2}{2\sigma^2}$.

Summarizing the above three cases, we have

$$\lambda_1=\begin{cases}\frac{\mu^2-x_0^2}{2\sigma^2}, & \frac{\sigma^2}{\mu(r-d)}\in(0,1),\\ \frac{\mu^2}{2\sigma^2}, & \frac{\sigma^2}{\mu(r-d)}=1,\\ \frac{\alpha_1^2\sigma^2}{2(r-d)^2}+\frac{\mu^2}{2\sigma^2}, & \frac{\sigma^2}{\mu(r-d)}\in(1,\infty),\end{cases}\quad\text{and}\quad \lambda_n=\frac{\alpha_n^2\sigma^2}{2(r-d)^2}+\frac{\mu^2}{2\sigma^2},\ \text{for}\ n\geq 2. \tag{3.15}$$

Moreover,

$$c_n=\frac{-\phi(v,\lambda_n)}{\lambda_n\phi_\lambda(d,\lambda_n)}=\frac{\sqrt{\mu^2-2\lambda_n\sigma^2}}{\mu-2\lambda_n(r-d)}\left[e^{\frac{-\mu^-(\lambda_n)}{\sigma^2}(v-d)}-e^{\frac{-\mu^+(\lambda_n)}{\sigma^2}(v-d)}\right],\quad n\geq 1. \tag{3.16}$$

Since $\alpha_n-\frac{2n-1}{2}\pi\to 0$ as $n\to+\infty$, we have the following asymptotic behaviors for λ_n and c_n:

$$\lambda_n\sim\frac{(2n-1)^2\sigma^2\pi^2}{8(r-d)^2}+\frac{\mu^2}{2\sigma^2}\sim\frac{(2n-1)^2\sigma^2\pi^2}{8(r-d)^2},\quad n\to+\infty, \tag{3.17}$$

$$\begin{aligned}c_n&\sim\frac{(-1)^{n+1}4(2n-1)\sigma^4\pi}{(2n-1)^2\sigma^4\pi^2+4\mu^2\sigma^2(r-d)^2-4\mu(r-d)}\\&\qquad\times e^{-\mu(v-d)/\sigma^2}\cos\left(\frac{(2n-1)\pi}{2}\times\frac{r-v}{r-d}\right)\\&\sim e^{-\mu(v-d)/\sigma^2}\frac{(-1)^{n+1}4}{(2n-1)\pi}\cos\left(\frac{(2n-1)\pi}{2}\times\frac{r-v}{r-d}\right),\quad n\to+\infty.\end{aligned} \tag{3.18}$$

Due to the above asymptotic behaviors for λ_n and c_n, we can differentiate (3.5) to obtain the density function of the hitting time. That is

Proposition 3.3. *The density function of the hitting time is give by*

$$p(t) := \frac{\mathbb{P}_v(\tau \in \mathrm{d}t)}{\mathrm{d}t} = \sum_{n=1}^{\infty} c_n \lambda_n e^{-\lambda_n t}, \quad t > 0. \tag{3.19}$$

The series in Proposition 3.3 is uniformly convergent on $[t_0, +\infty)$ for each $t_0 > 0$, while for small t the computational error may be very large (see Figures 4 and 5 below), we will give some details in the next section.

3.2. Hitting up

In this subsection, we deal with the case $d \in (v, r]$. In this case, we need to study the Sturm-Liouville (SL) equation $-\mathcal{G}u = \lambda u$ with the boundary condition $u'(0) = 0$. The unique (up to a multiple independent of x) non-trivial solution of this SL equation is:

$$\psi(x, \lambda) = \mu^+(\lambda) e^{\frac{-\mu^-(\lambda)x}{\sigma^2}} - \mu^-(\lambda) e^{\frac{-\mu^+(\lambda)x}{\sigma^2}}, \tag{3.20}$$

with $\mu^{\pm}(\lambda) := \mu \pm \sqrt{\mu^2 - 2\lambda\sigma^2}$. Moreover, if $\mu = 0$, $\psi(x, \lambda) = \cos\left(\frac{\sqrt{2\lambda}x}{\sigma}\right)$.
Again we have the following

Proposition 3.4. *The distribution of the hitting time is given by*

$$\mathbb{P}_v(\tau \le t) = 1 - \sum_{n=1}^{\infty} c_n e^{-\lambda_n t}, \quad t > 0, \tag{3.21}$$

where $0 < \lambda_1 < \lambda_2 < \cdots, \lambda_n \to \infty$ can be found as simple positive zeros of the function $\psi(d, \lambda)$, and c_n-s are given by $c_n = \frac{-\psi(v, \lambda_n)}{\lambda_n \psi_\lambda(d, \lambda_n)}$, $n = 1, 2, \ldots$. Moreover, it holds that $\sum_{n=1}^{\infty} c_n = 1$.

Remark 3.5. *If $\mu = 0$, the λ_n-s are given by $\lambda_n = \frac{(2n-1)^2 \sigma^2 \pi^2}{8d^2}$, and the c_n-s are given by $c_n = \frac{(-1)^{n+1} 4}{(2n-1)\pi} \cos\left(\frac{(2n-1)\pi v}{2d}\right)$. Thus we can differentiate (3.21) to obtain the density function.*

We next consider the case $\mu > 0$ (for the case $\mu < 0$, see Remark 3.6 below). Similarly as Subsection 3.1, by dealing with the equation $\psi(d, \lambda) = 0$ for $\lambda > 0$ in three different cases, we achieve the following (note that in this case, there is no root on $(0, \frac{\mu^2}{2\sigma^2})$)

$$\lambda_n = \frac{\alpha_n^2 \sigma^2}{2d^2} + \frac{\mu^2}{2\sigma^2}, \quad \text{for } n \ge 1, \tag{3.22}$$

where α_n is the unique root of the equation $\tan\alpha = -\frac{\sigma^2}{\mu d}\alpha$ in the interval $(\frac{2n-3}{2}\pi, (n-1)\pi]$ for $n \ge 1$. Moreover,

$$c_n = \frac{-\phi(v, \lambda_n)}{\lambda_n \phi_\lambda(d, \lambda_n)} = \frac{\sqrt{\mu^2 - 2\lambda_n \sigma^2}}{\mu + 2\lambda_n d} \left[e^{\frac{-\mu^-(\lambda_n)}{\sigma^2}(v-d)} - e^{\frac{-\mu^+(\lambda_n)}{\sigma^2}(v-d)} \right], \quad n \ge 1. \tag{3.23}$$

Since $\alpha_n - \frac{2n-3}{2}\pi \to 0$ as $n \to +\infty$, we have the following asymptotic behaviors for λ_n and c_n:

$$\lambda_n \sim \frac{(2n-3)^2\sigma^2\pi^2}{8d^2}, \quad c_n \sim e^{-\mu(v-d)/\sigma^2}\frac{(-1)^{n+1}4}{(2n-3)\pi}\cos\left(\frac{(2n-3)\pi v}{2d}\right), \quad n \to +\infty. \tag{3.24}$$

Due to the above asymptotic behaviors for λ_n and c_n, we can differentiate (3.21) to obtain the density function of the hitting time.

We conclude this section by the following remark concerning the case of $\mu < 0$.

Remark 3.6. *We can deal with the case of $\mu < 0$ by some simple transforms:*
(1) Hitting down: if $d \in [0, v)$, we can get the results through replacing μ, d and v by $-\mu$, $r-d$ and $r-v$ in the results in Subsection 3.2.
(2) Hitting up: if $d \in (v, r]$, we can get the results through replacing μ, d and v by $-\mu$, $r-d$ and $r-v$ in the results in Subsection 3.1.

4. Numerical illustration: convergence issues

This section presents some numerical experiments associated with the distribution function and the density function of the hitting time. We first study the hitting time density as the starting point v varies, and then investigate the convergence properties of the density function and the distribution function. We also make a comparison between the spectral expansion method and numerical Laplace inversion.

To get the distribution function and the density function of the first hitting time, we should first use the build-in function FindRoot in Mathematica to determine the roots of equation (3.10) (see also (3.13) and (3.14)), then compute the coefficients c_n-s by (3.16). Tables 1-4 report the values λ_n, c_n and $\sum_{i=1}^{n} c_i$ for different parameters. We find that in all of these cases the absolute values of c_n-s tend to zero as n increasing. In addition, the cumulative values of c_n tend to 1 as n increases. All of these observations are consistent with the theoretical results presented in Section 3 (see also Linetsky (2004*a*)).

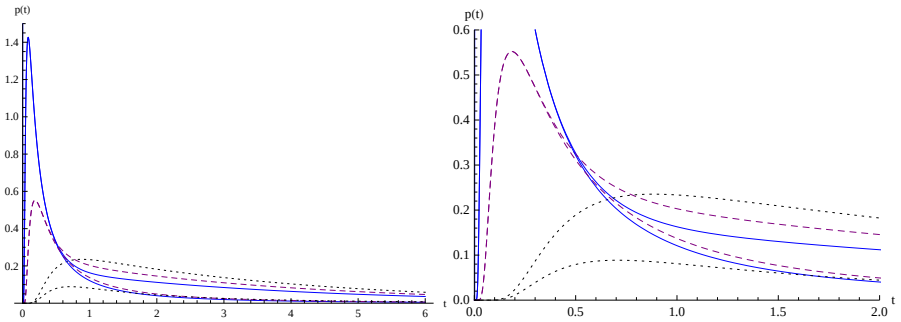

Figure 2: The density functions $p(t)$ of the hitting time. The solid, dashed and dotted lines correspond to different starting points $v = 1/2, 5/8, 1$, respectively. The lower one of each pair corresponds to the non-regulated version (see Footnote 4 below). The other parameters are $\mu = 1/4, \sigma = 1/2, d = 1/4, r = 1$.

Figure 2 depicts the density function of the hitting time with different starting points $v = 1/2, 5/8, 1$.[3] We find that when the hitting distance $v-d$ is small (large) the likelihood that the hitting point d is reached in a short term ($t<0.3$ for example) is large (small), while the long term ($t>1$ for example) density seems to be dominated by the case with large hitting distance. Note that in Figure 2, we also plot the corresponding density functions of hitting times for the non-regulated drifted Brownian motion. We find that, for small time, the density functions closely match their non-regulated versions, which is reasonable since, for small time, the likelihood of reflection is small. However, for large time, due to the effect of the reflection at the upper boundary, the density of the (downward) hitting time for the regulated version will be larger than that for non-regulated version.[4] Again these observations are accordant with intuition.

We next investigate the convergence properties for the density function and the distribution function. More precisely, we truncate the density function and the distribution function at the 80th, 100th, 200th and 500th term, respectively, and then compare their plots. Here we recall a theoretical result for the continuous diffusion (see, e.g., (15.1.1) in Karlin and Taylor (1981)):

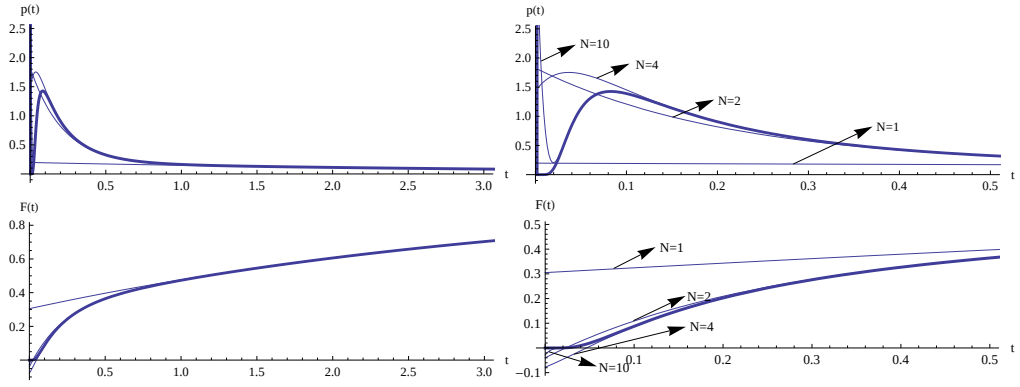

Figure 3: The density function $p(t)$ and the distribution function $F(t)$ of the hitting time with different N in (4.1). The plots in the right hand side are the local displays of the left ones. The thick lines correspond to

[3] Note that, from a practical point of view, it is not interesting to start a particle at the reflecting boundary, i.e., $v=1$ (since the particle cannot spend time on the reflecting boundary). We are very grateful to an anonymous referee for pointing out that. Here (and in Figures 4 and 5 below) we use a staring point $v=1$ mainly based on two aspects: one is the theoretical interest on the limiting behavior as $v=1$ (which is feasible, since the upper boundary is part of the domain; see, e.g., Section 15.6 in Karlin and Taylor (1981)); the other is that if we choose a starting point close to the upper boundary, say $v=0.999$ or $v=0.9999$, the numerical results will be virtually identical as those for $v=1$. The other parameters used in Figures 2, 4 and 5 are chosen just for convenience. In the next section, we will use some (economically or financially) reasonable parameters in applications.

[4] From p.363 in Karlin and Taylor (1975), it is easy to obtain the hitting time density for the drifted Brownian motion:

$$f_{nr}(t) = \frac{|d-v|}{\sqrt{2\pi t^3}} \exp\left\{-\frac{(d-v-\mu t)^2}{2t}\right\}, \quad \text{for } t \geq 0.$$

In fact, it is known that if $(d-v)\mu<0$, the above is a sub-density, which means that $\int_0^\infty f_{nr}(t)\mathrm{d}t<1$. While for $(d-v)\mu>0$, $f_{nr}(\cdot)$ is a conservative density (see Exercise 1.21 of Chapter VIII in Revuz and Yor (1999)).

the true functions (we view the functions in (4.1) with $N=500$ as the true functions). The other parameters are $v=1/2, \mu=1/4, \sigma=1/2, d=1/4, r=1$.

$$\lim_{h\downarrow 0}\frac{1}{h}\mathbb{P}_v(|X_h - v| > \varepsilon) = 0, \quad \text{for every } \varepsilon > 0.$$

(a) Using the first 80 eigenvalues.

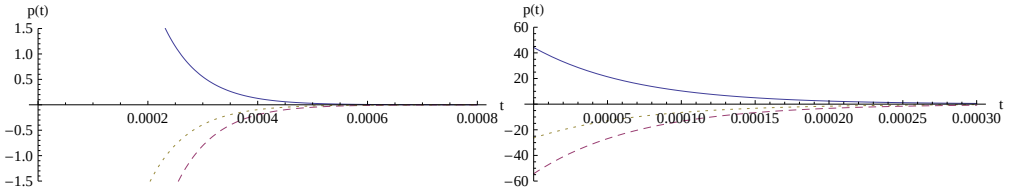

(b) Using the first 100 eigenvalues.

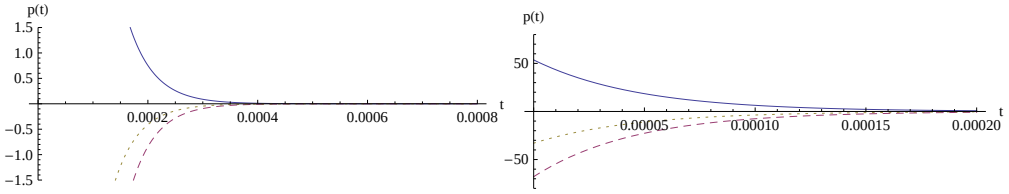

(c) Using the first 200 eigenvalues.

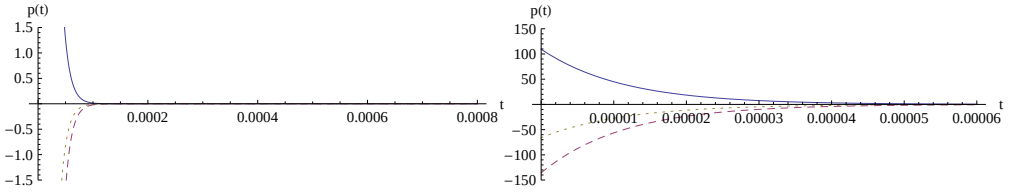

(d) Using the first 500 eigenvalues.

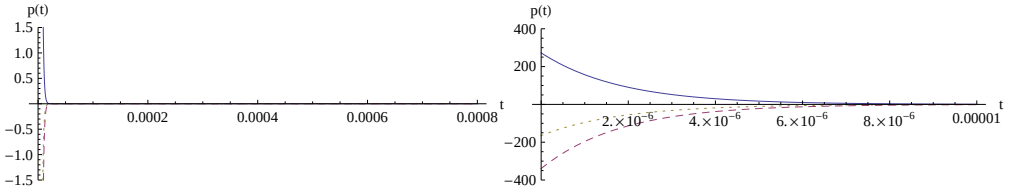

Figure 4: The convergence behavior of the density functions $p(t)$ of the hitting time. The solid, dashed and dotted lines correspond to different starting points $v=1/2, 5/8, 1$, respectively. The other parameters are $\mu=1/4, \sigma=1/2, d=1/4, r=1$.

From which one can see that the hitting time density should satisfy the property $p(t)\to 0$ as $t\downarrow 0$.[5] Despite it is well known that the convergence in eigenfunction expansion improves with

[5] In fact, for the standard Brownian motion, one can prove that (see also (2.8.5) in Karatzas and Shreve (1991))

$$p(t)/t \to 0, \quad \text{as} \quad t\downarrow 0.$$

the increasing of time (see, e.g., Linetsky (2004*a*)), we present some numerical results to make it convinced. Figure 3 plots the density and distribution functions truncated at different N:

$$p(t)=\sum_{n=1}^{N} c_n\lambda_n e^{-\lambda_n t},\ \ F(t)=1-\sum_{n=1}^{N} c_n e^{-\lambda_n t},\ \ t>0. \tag{4.1}$$

From Figure 3 we can see that, for time $t>1$, only the first term of the expansion is needed to make it virtually identical with the true function (here we use the truncated series with $N=500$). Moreover, when we add more and more terms into the series, the curve gets closer and closer to the true function. Specifically, on $t>0.03$, the curve with $N=10$ is virtually identical with the true function. Since the convergence behavior at large time scale is pretty good, next we are mainly concerned with the small time behavior. Figures 4 and 5 show these results. We find from Figure 4 that the more terms we used, the less the error at (relatively) large time (on $[0.0002,0.0008]$ for example), which is a desired property for computing these functions (see the left column in Figure 4). However, on the other hand, the absolute errors near time 0 become greater as we add more terms, which is a bothersome behavior for us (see the right column in Figure 4).

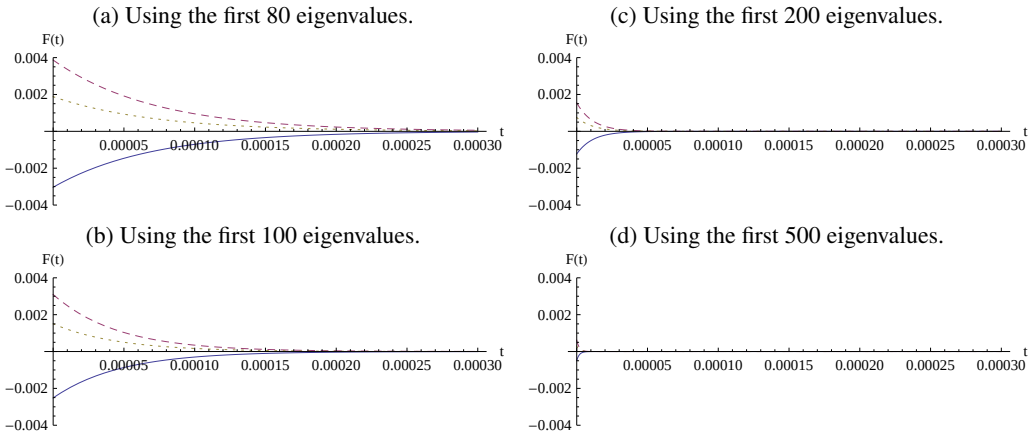

Figure 5: The distribution functions $F(t):=\mathbb{P}_v(\tau\le t)$ of the hitting time with different starting points $v=1/2,5/8,1$. The parameters are $\mu=1/4,\sigma=1/2,d=1/4,r=1$.

Now, the readers may wonder whether the integral errors will become large as we add more terms in calculating these functions. In fact, by some careful observations, we can also find in Figure 4 that the integral of the absolute value of the density function on the interval $[0,0.008]$ becomes small as we add more terms in the calculations. This can be verified by Figure 5 to some degree. From Figure 5, it can be find that the distribution function converges to zero at the small time scale, which is consistent with the theoretical results and the intuition. In the cases

under consideration, the errors are almost invisible when we use the 500-term truncation (see the last plot in Figure 5).

Table 1: The values of $\lambda_{n,d}$ and $c_{n,d}$ with the parameters $\mu=1/4,\ \sigma=1/2,\ d=1/4,\ r=1,\ v=1/2,\ \frac{\mu^2}{2\sigma^2}=1/8$ and $\frac{\sigma^2}{\mu(r-d)}=4/3$.

n	$\lambda_{n,d}$	$c_{n,d}$	$\sum_{i=1}^{n} c_{i,d}$
1	0.2836	0.6950	0.6950
2	4.7235	0.3450	1.0400
3	13.4984	0.1063	1.1463
4	26.6584	-0.0685	1.0777
5	44.2046	-0.1107	0.9670
6	66.1371	-0.0463	0.9207
7	92.4561	0.0374	0.9581
8	123.1616	0.0662	1.0243
9	158.2536	0.0297	1.0540
10	197.7320	-0.0257	1.0282

Table 2: The values of $\lambda_{n,d}$ and $c_{n,d}$ with the parameters $\mu=1/4,\ \sigma=1/4,\ d=1/4,\ r=1,\ v=1/2$ and $\frac{\sigma^2}{\mu(r-d)}=1/3,\ \frac{\mu^2}{2\sigma^2}=1/2$.

n	$\lambda_{n,d}$	$c_{n,d}$	$\sum_{i=1}^{n} c_{i,d}$
1	0.0051	0.8814	0.8814
2	1.4240	0.1296	1.0110
3	3.6019	0.0539	1.0649
4	6.8878	-0.0273	1.0376
5	11.2725	-0.0511	0.9864
6	16.7548	-0.0232	0.9633
7	23.3340	0.0163	0.9796
8	31.0101	0.0310	1.0107
9	39.7829	0.0146	1.0253
10	49.6523	-0.0116	1.0137

Table 3: The values of $\lambda_{n,d}$ and $c_{n,d}$ with the parameters $\mu=1/4,\ \sigma=\sqrt{3}/4,\ d=1/4,\ r=1,\ v=1/2,\ \frac{\mu^2}{2\sigma^2}=1/6$ and $\frac{\sigma^2}{\mu(r-d)}=1$.

n	$\lambda_{n,d}$	$c_{n,d}$	$\sum_{i=1}^{n} c_{i,d}$
1	0.1667	0.6667	0.6667
2	3.5318	0.4339	1.1006
3	10.1133	0.1289	1.2295
4	19.9833	-0.0968	1.1327
5	33.1430	-0.1425	0.9906
6	49.5924	-0.0600	0.9305
7	69.3317	0.0477	0.9782
8	92.3608	0.0650	1.0433
9	118.6797	0.0383	1.0716
10	148.2886	-0.0429	1.0387

Table 4: The values of $\lambda_{n,d}$ and $c_{n,d}$ with the parameters $\mu=0,\ \sigma=1/2,\ d=1/4,\ r=1$ and $v=1/2$. Recall the results in Remark 3.2.

n	$\lambda_{n,d}$	$c_{n,d}$	$\sum_{i=1}^{n} c_{i,d}$
1	0.5483	0.6366	0.6366
2	4.9348	0.4244	1.0610
3	13.7078	0.1273	1.1884
4	26.8763	-0.0909	1.0974
5	44.4132	-0.1415	0.9559
6	66.3457	-0.0579	0.8981
7	92.6646	0.0490	0.9470
8	123.3701	0.0849	1.0319
9	158.4620	0.0374	1.0694
10	197.9404	-0.0335	1.0359

Table 5: The total CPU times (in seconds) costed by spectral expansion and Laplace inversion for computing the hitting time density at $t=0.001,0.002,0.003,\ldots,1$. The parameters are $v=1/2,\mu=1/4,\sigma=1/2,d=1/4,r=1$. We use the Gaver-Stehfest algorithm (see Abate and Whitt (1992), Valkó and Vajda (2002) and Abate and Valkó (2004) for the other algorithms for inverting the Laplace transform) used in Kou and Wang (2003) to invert the Laplace transform. We report (in parenthesis) the required number N in (4.1) to achieve the respective accuracy for the spectral expansion approach. For the Laplace inversion approach, we set the burning-out number as 2 and use the M-point Richardson extrapolation (see also Section 5 in Kou and Wang (2003)). We also report the minimal value of M that can achieve the required accuracy in parenthesis. The program is coded by MATHEMATICA® and is performed on a laptop (Intel Core i5-520, 2.4 GHz processor and 4GB of RAM).

Method\Accuracy	10^{-3}	10^{-4}	10^{-5}
Laplace Inversion	36.86 (10)	45.91 (13)	58.45 (15)
Spectral Expansion	1.62 (73)	1.83 (80)	2.04 (88)

At last, we consider the required computational time of the spectral method. Since the problem (3.10) has been transformed into solving some elementary equations (3.13) and (3.14), this

work (finding the first 500 eigenvalues for example) can be done in several seconds. Moreover, compared with the numerical Laplace inversion method (which can only calculate the density function point by point), we can obtain the whole density function at one time (the only drawback is the error in the small time scale, which is always not important in applications in economics, finance and other application fields). According to our experience, within the time costed by finding the first hundreds of eigenvalues, we can only obtain the density values at several time points by using Laplace inversion. Table 5 reports some related results,[6] which show that in order to achieve the accuracy up to five decimal points for the hitting time density $p(t)$ at time $t = 0.001, 0.002, 0.003, \ldots, 1$, by the spectral expansion method, we need to compute the first 88 terms, which spends about 2 seconds. While the Laplace inversion approach will cost about one minute to achieve the some accuracy. In conclusion, when we concern the computational issues for the density of the hitting time for reflected Brownian motion, the spectral expansion approach is more superior than the numerical Laplace inversion method.

5. Applications in insurance and finance

In this section, we present two applications of our main results: one is to compute the bankrupt probability for an insurance company; the other is to price a corporate (defaultable) bond, which is important in finance, especially in credit (default) risk.

5.1. Computing the bankrupt time distribution for an insurance company

In this subsection, we follow the setting in Gerber and Shiu (2004): we model the (pre-dividend) surplus of an insurance company by a Wiener process (or Brownian motion) with positive drift:

$$Y_t = v + \mu t + \sigma W_t, \quad t \geq 0, \tag{5.1}$$

where $v > 0$ is the initial surplus, $\mu > 0$, $\sigma > 0$ and W is a standard Winer process. The dividends are paid according to a barrier strategy with parameter $r > v$: whenever the (regulated) surplus reaches the level r, the "overflow" is paid as dividends to shareholders. If we define the running maximum by $M_t := \max_{0 \leq s \leq t} Y_s$, the aggregate dividends paid by time t are $U_t := (M_t - r)^+ :=$

[6] It is not hard to obtain the Laplace transform of τ by adopting the method used in Bo, Zhang and Wang (2006) and Bo, Wang and Yang (2011):

$$g(\lambda; v, d) := \mathbb{E}_v\left[e^{-\lambda\tau}\right] = \frac{\mu^+ e^{\frac{\mu^-(1-v)}{\sigma^2}} - \mu^- e^{\frac{\mu^+(1-v)}{\sigma^2}}}{\mu^+ e^{\frac{\mu^-(1-d)}{\sigma^2}} - \mu^- e^{\frac{\mu^+(1-d)}{\sigma^2}}}, \text{ with } \mu^\pm = \mu \pm \sqrt{\mu^2 + 2\lambda\sigma^2}. \tag{4.2}$$

$\max\{M_t - r, 0\}$. Now the post-dividend (regulated) surplus process should be

$$X_t = Y_t - U_t, \ \ t \geq 0. \tag{5.2}$$

Since $L_0 = 0$ and L increases only when $X = 0$, we have that U is (pathwise) identical with the upper regulator in (2.1) before the first hitting time to zero:

$$\tau_0 := \inf\{t \geq 0 : X_t - U_t = 0\}. \tag{5.3}$$

Also it is not hard to see that τ_0 has the same distribution as τ defined in (3.1) with $d = 0$ (see (3.7) in Gerber and Shiu (2004) for the Laplace transform of τ_0, and compare it with (4.2) in our paper). Thus we can compute the distribution of the above hitting time τ_0 by applying the results in Subsection 3.1. Figure 6 shows some numerical results, from which we can find that the insurance company will bankrupt with probability 0.5 within forty years, and the likelihood that the company will be alive after two-hundred years is less than 5 percent.

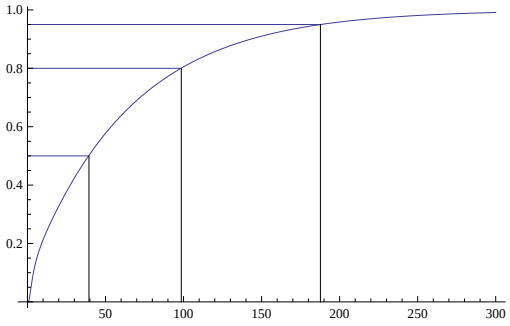

Figure 6: The cumulate distribution function of τ_0. The model parameters are $v = 1/2, \mu = 1/20, \sigma = 1/5, r = 1$.

5.2. Pricing the zero-recovery corporate (defaultable) bond

In this section, we model the asset return process of a firm by the reflected process (see also Veestraeten (2008) and Bo et al. (2010)) in (2.1). Then the market value of the firm can be specified as

$$S_t = e^{X_t}, \ \ t \geq 0. \tag{5.4}$$

Following the pioneering work by Black and Cox (1976), we define the default time by the following first passage time:

$$\tau_D := \inf\{t \geq 0 : S_t \leq D\}, \tag{5.5}$$

with $D \in (0, S_0)$ being the default barrier. Then the time-zero price of a zero-coupon zero-recovery corporate bond with face value 1 and maturity date T is given by

$$P(T;D) := \mathbb{E}\left[e^{-RT}\mathbf{1}_{\{\tau_D > T\}}\right] = e^{-RT}\mathbb{P}(\tau_D > T), \tag{5.6}$$

where $R > 0$ is the risk-free interest rate. Note that $X_t = \ln S_t$, then it follows that τ_D has the same distribution as τ given in (3.1) with $d = \ln D$. Thus we can compute the price $P(T;D)$ by using the results in Subsection 3.1. Figure 7 depicts the prices of the defaultable bond as well as a risk-free bond as functions of the maturity time T. Due to the default risk, the price of the defaultable bond should be lower than that for the risk-free bond.

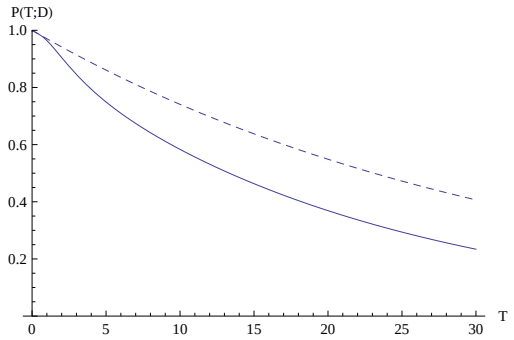

Figure 7: The price of the zero-recovery defaultable bond with $S_0 = e^{1/2}$, $r = 1$ and $D = e^{1/4}$. The other parameter values are $R = 3/100, \mu = 1/20, \sigma = 1/5$, which are widely used in financial literature. The dashed curve is the price of a risk-free bond with face value 1, i.e., e^{-RT}.

6. Conclusion

In this paper, we have presented the detailed analysis on the computational issues on the spectral representation for the hitting time density of the reflected Brownian motion with two-sided barriers. The problem of finding the eigenvalues is transformed into solving some elementary equations (which are pretty simple). We provided some numerical analysis on the properties of the hitting time density and the convergence behaviors of the spectral expansion formulas for the density function and the distribution function. Numerical results reveal that, specialized on the reflected Brownian motion case, the spectral representation is more appealing than the method of numerical Laplace inversion. Two applications (one in insurance theory, the other in credit risk) of the main results have been included.

Acknowledgement

The authors would like to thank an anonymous referee for valuable comments and suggestions which helped to improve the paper significantly. This work was supported by the LPMC at

Nankai University and the Keygrant Project of Chinese Ministry of Education (No. 309009).

References

Abate, J. and PP Valkó. 2004. "Multi-precision Laplace transform inversion." *Int. J. Numer. Meth. Engng* 60(5):979–993.

Abate, J. and W. Whitt. 1992. "The Fourier-series method for inverting transforms of probability distributions." *Queueing Systems* 10(1):5–87.

Black, F. and J.C. Cox. 1976. "Valuing corporate securities: Some effects of bond indenture provisions." *Journal of Finance* 31(2):351–367.

Bo, L., D. Tang, Y. Wang and X. Yang. 2010. "On the conditional default probability in a regulated market: a structural approach." *Quantitative Finance, DOI: 10.1080/14697680903473278* .

Bo, L., L. Zhang and Y. Wang. 2006. "On the first passage times of reflected OU processes with two-sided barriers." *Queueing Systems* 54(4):313–316.

Bo, L., Y. Wang and X. Yang. 2010. "On the conditional default probability in a regulated market with jump risk." *Preprint* .

Bo, L., Y. Wang and X. Yang. 2011. "Some integral functionals of reflected SDEs and their applications in finance." *Quantitative Finance* 11(3):343–348.

Bo, L., Y. Wang, X. Yang and G. Zhang. 2011. "Maximum likelihood estimation for reflected Ornstein-Uhlenbeck processes." *Journal of Statistical Planning and Inference* 141(1):588–596.

Gerber, H.U. and E.S.W. Shiu. 2004. "Optimal dividends: analysis with Brownian motion." *North American Actuarial Journal* 8(1):1–20.

Harrison, J.M. 1978. "The diffusion approximation for tandem queues in heavy traffic." *Advances in Applied Probability* 10(4):886–905.

Harrison, JM. 1985. *Brownian Motion and Stochastic Flow Systems*. Wiley: New York.

Karatzas, I. and S.E. Shreve. 1991. *Brownian Motion and Stochastic Calculus*. Springer.

Karlin, S. and H.M. Taylor. 1975. *A First Course in Stochastic Processes*. Academic press.

Karlin, S. and H.M. Taylor. 1981. *A Second Course in Stochastic Processes*. Academic press.

Kent, J.T. 1980. "Eigenvalue expansions for diffusion hitting times." *Probability Theory and Related Fields* 52(3):309–319.

Kent, J.T. 1982. "The spectral decomposition of a diffusion hitting time." *The Annals of Probability* 10(1):207–219.

Kou, S.G. and H. Wang. 2003. "First passage times of a jump diffusion process." *Advances in Applied Probability* 35(2):504–531.

Linetsky, V. 2004*a*. "Computing hitting time densities for CIR and OU diffusions: applications to mean-reverting models." *Journal of Computational Finance* 7:1–22.

Linetsky, V. 2004*b*. "Lookback options and diffusion hitting times: a spectral expansion approach." *Finance and Stochastics* 8(3):373–398.

Linetsky, V. 2005. "On the transition densities for reflected diffusions." *Advances in Applied Probability* 37(2):435–460.

McKean, H.P. 1956. "Elementary solutions for certain parabolic partial differential equations." *Transactions of the American Mathematical Society* 82(2):519–548.

Revuz, D. and M. Yor. 1999. *Continuous Martingales and Brownian Motion*. Springer Verlag.

Valkó, P.P. and S. Vajda. 2002. "Inversion of noise-free Laplace transforms: towards a standardized set of test problems." *Inverse Problems in Science and Engineering* 10(5):467–483.

Veestraeten, D. 2004. "The conditional probability density function for a reflected Brownian motion." *Computational Economics* 24(2):185–207.

Veestraeten, D. 2008. "Valuing stock options when prices are subject to a lower boundary." *Journal of Futures Markets* 28(3):231–247.

Werner, W. 1995. "Some remarks on perturbed reflecting Brownian motion." *Séminaire de Probabilités XXIX* pp. 37–43.

Williams, R. J. 1992. "Asymptotic variance parameters for the boundary local times of reflected Brownian motion on a compact interval." *Journal of Applied Probability* 29(4):996–1002.